


Model-Driven Deep Learning OAMP Detection Based on LDPC for Scalable Massive MIMO Systems

Saja Abdul Karim Anwar^{1*}, and Marwa Al-Sultani² 

¹Department of Communication Engineering, College of Engineering, University of Diyala, Iraq; Email: eng_grad_communication2505@uodiyala.edu.iq

²Department of Communication Engineering, College of Engineering, University of Diyala, Iraq; Email: eng85marwa@gmail.com

*Correspondence: Saja Abdul Karim Anwar, eng_grad_communication2505@uodiyala.edu.iq

ABSTRACT- The paper analyzes the performance of Massive MIMO system with LDPC code. Utilizing the benefit of the power of model driven deep learning, which is a deep learning technique whose main characteristic is to maintain the mathematical structure of the model, converting the iterative detector into a neural network by making the parameters learnable rather than fixed. This method requires less data and has a faster training rate. This learning technique is used in order to enhance the output of the detector and thereby enhance the output of the LDPC decoder. The simulation outcomes reveal the strength of integrating both OAMP-NET detector with LDPC to scalable massive MIMO systems with different antenna configurations ranging from 4×4 to 64×64. The proposed system OAMP-NET+LDPC achieves a significant improvement in detection performance in both perfect and imperfect CSI scenarios. In addition, we conducted a comprehensive analysis of scalability and computational complexity to evaluate its practical feasibility for different MIMO configurations. In addition, we conducted generalization experiments under unseen SNR conditions and variable channel correlations, in addition to ablation studies at the depth of the unfolded network to prove the robustness and effectiveness of the proposed system.

Keywords: BER, LDPC Code, Massive MIMO, Model Driven Deep Learning, OAMP, OAMP-NET.

ARTICLE INFORMATION

Author(s): Saja Abdul Karim Anwar, and Marwa Al-Sultani;

Received: 11/03/26; **Accepted:** 02/06/26; **Published:** 30/06/26;

E- ISSN: 2347-470X;

Paper Id: IJEER 1103B12;

Citation: 10.37391/ijeer.140229

Webpage-link:

<https://ijeer.forexjournal.co.in/archive/volume-14/ijeer-140229.html>



Publisher's Note: FOREX Publication stays neutral with regard to jurisdictional claims in Published maps and institutional affiliations.

1. INTRODUCTION

The Massive multiple-input multiple-output technology (MIMO) has many benefits, including an enhancement in the network capacity and spectral efficiency and reliability that are essential in beyond fifth-generation (B5G) wireless networks [1, 2]. Nevertheless, the computational requirements of massive MIMO detectors are increased as the number of antennas used grows, and therefore, the traditional data detection methods are not applicable in large-scale MIMO systems [3, 4]. Deep learning (DL) belongs to the most promising technologies in artificial intelligence (AI) that used in wireless communication systems application [5]. It is capable of being trained well to estimate the signal vectors being transmitted. The detectors of DL based were applied to achieve the optimal performance with minimum complexity [4]. Nevertheless, deep learning approaches based on data are usually memory and time-intensive, and thus they may not be applicable in practice [6].

In order to overcome these drawbacks, model-driven deep learning has been suggested as a perspective that incorporates expert experience and mathematical formulations into the network structure. In this method, the network topology is built by unfolding or parameterizing known iterative algorithms and produces architectures that are easier to train and interpretation than data driven models, and depends on data-based optimization[7]. In this sense, orthogonal approximate message passing (OAMP) has been generalized into a trainable model called OAMP-Net where some of the algorithmic parameters can be trained and optimized through deep learning. MIMO massive detector OAMP-Net has received great attention because of the fact that it has low training overhead, rapid convergence, and it also has a natural provision of soft symbol -level and reliability that is used by soft demodulator to produce LLRs to use in iterative or soft input channel decoding of the modern wireless system [8].

Along with the developments in multi-antenna signal processing, channel coding remains a fundamental part of providing reliability in the 5G network [9]. The LDPC codes are well-known with their high error-correction ability and their ability to be used in a high-throughput environment [10]. Therefore, LDPC decoding is scientifically attractive, especially in systems with high data rates, including massive MIMO, where the coding performance is directly affected by the reliability of the soft information output by the detector. Thus, OAMP-Net and LDPC coding can be combined to achieve a significant improvement in performance of the BER,

as evidenced by the fact that BER dropped substantially throughout the whole SNR space. To minimize this error propagation an LDPC decoder is added to offset any residual detection error and therefore keep the performance constant. Therefore, wideband MIMO systems are highlighting the benefits of integrating LDPC.

Although deep unfolding detectors such as OAMP-NET have shown promising performance in MIMO systems, most existing studies focus on small-scale configurations under perfect CSI assumptions with limited scalability and robustness analysis. Based on these limitations, this work presents a scalable LDPC-encoded OAMP NET framework for massive MIMO systems under both perfect and imperfect CSI conditions, with an emphasis on scalability, robustness, parameter efficiency across different antenna dimensions.

The main contributions and research novelty of this work can be summarized as follows:

- We developed a scalable LDPC-encoded OAMP-NET framework for detecting massive MIMO signals, which we evaluated coherently across antenna dimensions ranging from 4×4 to 64×64 without architectural reconfiguration or parameter rescaling.
- We conducted a comparison between conventional detectors and deep learning-based detectors and demonstrated the effectiveness of the proposed system model.
- We conducted a comprehensive robustness analysis of the system under both perfect and imperfect CSI assumptions.
- We show that the model-driven deep learning detector achieves competitive (BER) performance while maintaining very low trainable complexity by using only 20 learnable parameters, making it suitable for scalable massive MIMO applications.
- We present a detailed analysis of convergence, complexity, scalability, generalization analysis and ablation study in deep learning-based MIMO detection systems.

The research will be organized as following: the second section provides the related work, third section presents the proposed system model, fourth section shows the simulation results and discussion, and finally, five section provides research's conclusion.

2. RELATED WORK

In [11], the authors investigated massive MIMO systems encoded with LDPC technology and combined with NOMA techniques to improve spectrum efficiency and BER performance in 5G communications. However, this work assumes ideal channel estimation and relies only on traditional detection methods without incorporating deep learning or model-driven iterative detectors, the analysis mainly focuses on BER performance and complexity reduction without considering robustness under imperfect CSI, scalability across different MIMO dimensions.

In [12] the authors investigated massive MIMO systems encoded with LDPC technology using low-complexity detectors based on the MMSE-PIC algorithm and its variants. However, the work was limited to conventional MMSE-based detectors and Deep learning techniques have not been studied. Additionally, the imperfect CSI and scalability across different MIMO dimensions and hybrid LDPC-deep learning frameworks have not been investigated,

Waheed et al. in [10] studied OTFS-modulated massive MIMO system combined with 5G NR LDPC coding to enhance BER performance, spectrum efficiency, and communication robustness in high mobility scenarios. However, the study relies mainly on conventional detectors such as (MPA and LMMSE) and does not study deep learning techniques or Model-driven detection techniques. Additionally, the evaluation is limited to fixed system settings without analyzing scalability across different MIMO dimensions, parameter efficiency, or robustness under imperfect CSI condition.

In [13] the authors proposed a DNN-based 5G MIMO communication system integrating deep neural networks (DNN) with LDPC and polar coding to improve the bit error rate (BER) performance and spectrum efficiency in flat fading channel conditions. However, the study was limited to a 4×16 fixed MIMO configuration and employed a conventional LMMSE equalizer instead of model-driven deep learning detectors. Additionally, scalability across massive MIMO dimensions and robustness under imperfect CSI conditions and comprehensive complexity analysis have not been investigated.

3. PROPOSED SYSTEM MODEL

Figure 1 illustrates the system model, the proposed receiver structure integrates massive MIMO, LDPC channel coding, and deep learning-based detection to allows high-throughput and reliable wireless transmission under practical channel impairments. At the transmitter, the system was employing a large-scale antenna array at the base station, massive MIMO leverages spatial diversity and array gain to suppress multiuser interference and enhance link robustness.

At the receiver, a deep learning-assisted MIMO detector is employed to recover the transmitted symbol vector from the high-dimensional signal received, the proposed detector is designed to provide improved performance-complexity trade-offs by learning critical parameters from data while preserving the iterative structure of model-based detection algorithms. Notably, the detector is designed to generate soft symbol level outputs as well as reliability information, making it suitable for modern coding systems. The detector outputs are subsequently processed by a soft demodulation stage to produce LLRS log-likelihood ratios, which are fed to the LDPC decoder, enabling efficient error correction and resulting in the final recovered bit stream.

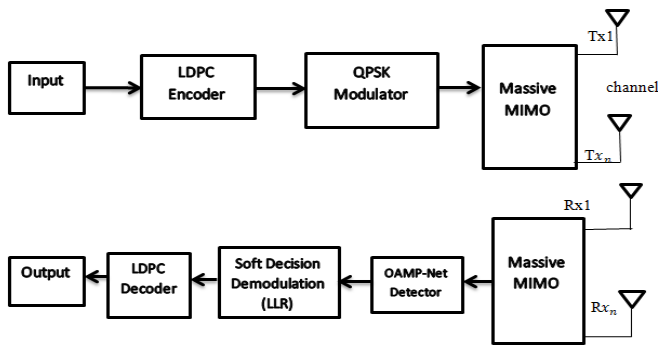


Figure 1. The system mode

3.1. Massive MIMO

In a massive MIMO system uplink, the base station receives the signal vector y by N antennas serving K single-antenna users and is expressed as:

$$y = Hx + n \quad (1)$$

where $y \in \mathbb{C}^{N \times 1}$ is the received signal vector, $H \in \mathbb{C}^{N \times K}$ channel matrix, in which each element of which is the channel gain between a base station antenna and user, $x \in \mathbb{C}^{K \times 1}$ is the transmitted signal vector by the K users, and $n \in \mathbb{C}^{N \times 1}$ is the base station Gaussian noise. In the case of the downlink transmission (from the base station to the users), the signal transmitted by the base station is represented as x and the signal will be of the form:

$$x = Ws \quad (2)$$

Where $W \in \mathbb{C}^{N \times K}$ is the matrix of the precoding, s is the transmitted symbol vector. The signal received at the K users is:

$$r = H^T x + n \quad (3)$$

Where r is the received signal vector, H^T is the transpose of the channel matrix H , x is the transmitted signal vector, n is the additive white Gaussian noise vector. Effects that are usually included in the channel matrix H include path loss and fading and is expressed as:

$$H = GD \quad (4)$$

where $G \in \mathbb{C}^{N \times K}$ represents the matrix of the small-scale fading, and $D \in \mathbb{R}^{K \times K}$ is the diagonal matrix which represents large-scale fading [13].

3.2. Model-Driven DL Detector

We introduce the OAMP and OAMP -NET structure.

3.2.1. OAMP Detector

The algorithm OAMP has been suggested to solve the problems of sparse linear inverse in compressed sensing and can be applied in Massive MIMO detection in *algorithm 1* [7]. The algorithm targets the recovery of the transmitted signal vector x_d using the received signal vector;

$$y_d = Hx_d + n_d$$

where x_d is the transmitted signal vector, y_d is the received signal vector, H is the channel matrix between transmit and receive antennas, n_d is the additive white Gaussian noise (AWGN) [7].

Algorithm 1: Massive MIMO Detection by using OAMP Algorithm

Input: The matrix of channel estimated \hat{H} , Received signal y_d , The matrix of equivalent noise covariance $R_{\hat{n}d\hat{n}d}$.

Output: The signal Recovered $\hat{x}_d, T+1$.

Initialize: $\tau l \leftarrow 1, \hat{x}_d, 1 \leftarrow 0$

$$r_t = \hat{x}_{d,t} + W_t(y_d - \hat{H}\hat{x}_{d,t}) \quad (5)$$

Where r_t is the intermediate residual estimate at iteration t , $\hat{x}_{d,t}$ is the estimated transmitted signal vector at iteration t , W_t is the linear estimation matrix (or weighting matrix) at iteration t , y_d is the received signal vector, $\hat{H}\hat{x}_{d,t}$ is the residual error between the received signal and the reconstructed signal.

$$\hat{X}_{d,t+1} = E[x|r_t, \tau_t] \quad (6)$$

Where $\hat{X}_{d,t+1}$ the estimated transmitted signal vector at iteration $t+1$, E is the conditional expectation operator, r_t is the residual estimate obtained from the linear estimation stage, τ_t variance at iteration t .

$$v_t^2 = \frac{\|y_d - \hat{H}\hat{x}_{d,t}\|_2^2 - \text{tr}(R_{\hat{n}d\hat{n}d})}{\text{tr}(\hat{H}^H\hat{H})} \quad (7)$$

Where v_t^2 is the estimated variance at iteration t , \hat{H} is the estimated channel matrix, $R_{\hat{n}d\hat{n}d}$ is the covariance matrix of the estimated noise component, tr is the matrix trace

$$\tau_t^2 = \frac{1}{N_t} \text{tr}(B_t B_t^H) v_t^2 + \frac{1}{N_t} \text{tr}(W_t R_{\hat{n}d\hat{n}d} W_t^H) \quad (8)$$

Where τ_t^2 is the estimated error variance at iteration t , N_t is the number of transmit antennas, B_t is the residual transformation matrix at iteration t , W_t is the linear estimation matrix, tr is the matrix trace.

Algorithm 1 listed the OAMP detector and primarily includes two modules: linear estimator *eq. (5)* and nonlinear estimator *eq. (6)*, the algorithm discussed in detail in [7].

3.2.2 OAMP-Net detector

The OAMP-Net has the structure shown in *figure 2*, which is an algorithmic extension of algorithm with addition of learnable scalar variables γ_t and θ_t . The network is comprises of T cascade layers and the structure of each layer is identical that includes the MMSE denoiser, the tied weights and the error variance τ_t^2 . Initial value $\hat{x}_1 = 0$ and Received signal y and are the input of the OAMP-Net and the ultimate estimate \hat{x}_{T+1} of signal x is the output. In the t^{th} layer of the OAMP-Net, the input is the estimated signal $\hat{x}_{t,d}$ of the $(t-1)^{\text{th}}$ layer and the received signal y_d . The only distinction between the OAMP algorithm and OAMP-Net is the learnable variables (γ_t, θ_t) , which are essential in the network. OAMP algorithm

is based on the assumption that $\gamma_t = \theta_t = 1$ to make q_t and h_t orthogonal. Since the role of the variables that are learnable (γ_t, θ_t) is to provide the correct step sizes to update the variance and mean during the MMSE denoiser, we are supposed to achieve optimal variables (γ_t, θ_t), by deep learning. The OAMP-Net algorithm discussed in detail in [7].

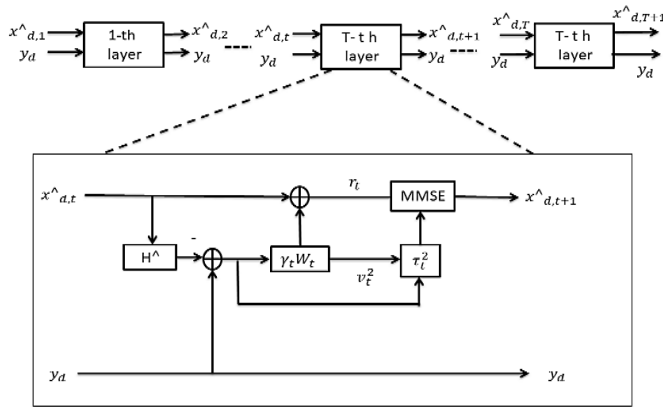


Figure 2. The OAMP-Net architecture

3.3. LDPC Coded OAMP-Net Detector for Massive MIMO

The LDPC code is provided as a matrix representation $[G, H]$ with G being the generator matrix of the code and H being the parity check matrix (PCM). The parity matrix H is not dense, having just a few ones. It may be depicted as a Tanner graph. This is a graph that is composed of two categories of nodes: check nodes (CNs) and bit nodes (BNs) connected with the help of edges [14].

Algorithm 2 summarizes the proposed LDPC-coded OAMP - NET detector. The method first begins by performs iterative OAMP-based symbol estimation using trainable parameter γ_t, θ_t , followed by MMSE denoising. After that soft output LLR values are generated and passed to the LDPC decoder to improve BER performance in massive MIMO systems.[7,8].

Algorithm 2: Proposed LDPC-Coded OAMP-Net

Input : Received signal y , Estimated channel matrix \hat{H} , Noise variance σ^2 , Constellation symbols S , Number of OAMP-Net layers T , LDPC parity-check matrix H .

Output: Estimated transmitted symbols \hat{x} , Decoded information bits \hat{b} .

Initialization: 1- Set initial estimate $\hat{x}(0) = 0$, 2- Initialize trainable parameters $\gamma_t = \theta_t = 1$

For $t = 1$ to T do :

Step 1: Compute residual error $e_t = y - \hat{H}\hat{x}(t)$ (9)

Where e_t is residual error vector at iteration t

Step 2: Estimate residual variance $v_t^2 = \frac{\|e_t\|^2 - N_r \sigma^2}{\text{tr}(\hat{H}^T \hat{H})}$ (10)

Where v_t^2 is estimated error variance at iteration t , N_r is number of receive antennas.

Step 3: Compute LMMSE matrix

$$\hat{W}_t = v_t^2 \hat{H}^T (v_t^2 \hat{H} \hat{H}^T + \sigma^2 I)^{-1} \quad (11)$$

Where \hat{W}_t is estimated linear MMSE filtering matrix at iteration t , I is Identity matrix.

Step 4: Apply de-correlation normalization

$$W_t = \frac{N_t}{\text{tr}(\hat{W}_t \hat{H})} \hat{W}_t \quad (12)$$

Where N_t is the number of transmitted antenna

Step 5: Perform linear estimation

$$r_t = \hat{x}_t + \gamma_t W_t (y - \hat{H} \hat{x}_t) \quad (13)$$

Where r_t is the pseudo-observation vector, γ_t is trainable scaling parameter at iteration t

Step 6: Estimate effective noise variance

$$\tau_t^2 = \frac{\text{tr}(c_t c_t^T) v_t^2}{N_t} + \frac{\theta_t^2 \sigma^2 \text{tr}(W_t W_t^T)}{N_t} \quad (14)$$

Where τ_t^2 is equivalent noise variance at iteration t , c_t is residual transformation matrix, typically defined as $c_t = I - \theta_t W_t \hat{H}$, θ_t is trainable scaling parameter at iteration t .

Step 7: Apply MMSE denoiser

$$\hat{x}_{(t+1)} = E\{x | r_t, \tau_t^2\} \quad (15)$$

Where $\hat{x}_{(t+1)}$ is the updated estimate of the transmitted symbol vector at iteration $t+1$, $E\{x | r_t, \tau_t^2\}$ is posterior mean estimator (MMSE denoiser)

Step 8: Obtain final detected symbols

$$\hat{x} = \hat{x}(T) \quad (16)$$

Step 9: Generate soft-output LLR values

$$LLR = \log \left[\frac{p(\text{bit}=0 | \hat{x})}{p(\text{bit}=1 | \hat{x})} \right] \quad (17)$$

Where LLR is Log-Likelihood Ratio, $p(\text{bit} = 0 | \hat{x})$ Posterior probability that the transmitted bit is 0 given the estimated symbol x , $p(\text{bit} = 1 | \hat{x})$ is Posterior probability that the transmitted bit is 1 given the estimated symbol x .

Step 10: Perform LDPC belief propagation decoding

$$\hat{b} = \text{LDPC decoder}(LLR) \quad (18)$$

Return: Estimated symbols \hat{x} , Decoded bits \hat{b}

4. SIMULATION RESULTS AND DISCUSSION

This section presents an evaluation of the performance of the studied MIMO signal detection methods under both perfect and imperfect channel state information (CSI). The analysis includes BER performance, computational complexity, convergence behavior, and robustness across different antenna configurations. In addition, it presents generalization analysis and statistical validation to evaluate the reliability of the obtained results. All simulations were implemented using the Python language and were evaluated for MIMO configurations ranging from 4×4 to 64×64 within the SNR range of 0-20dB.

Simulation Parameters

Modulation scheme: QPSK modulation scheme.

Channel Model: Rayleigh fading (i.i.d)

CSI Condition: Perfect and Imperfect CSI

Channel estimation error :0.05

Min Bit Errors: 1000

Massive MIMO configurations: 4×4 , 8×8 , 16×16 , 32×32 , 64×64

Packages: PyTorch + Numpy + pyldpc

Data generation process:

- The received Massive MIMO signals which are to be used as a dataset are simulated as the transmission $y=Hx+n$ and multiple SNR (noise) condition.
- The received symbols in a Massive MIMO system of configuration (4×4 , 8×8 , 16×16 , 32×32 , 64×64) with a normalized fading channel and complex AWGN noise are used as the input data.
- The labels are the respective transmitted symbols of the supervised learning of the detector (OAMP-Net).
- To assess the performance of the models, the dataset was divided into 80% to be used in training and 20% to be used in validation / testing.

SNR range: 0 – 20 dB

OAMP Iterations / OAMP- Net layers: 10

DetNet layers: 12

DetNet hidden dimension: 96

Training samples: 100000

OAMP-Net Training epochs: 50

DetNet epoch: 60

Batch sizes: 50

Learning rate: 0.001

Max Symbol Per SNR: 500000

Optimizer: Adam

Early stopping patience: 10

Learnable parameters: OAMP – Net parameters = 20, (θ, γ) for each layer

Dropout rate: 0.1

LDPC parameters: code word length = 96, Variable node degree=3, check node degree=6

LDPC decoding: Belief propagation

Sphere max exact real dim: 2^*N_{tx}

Sphere K-bset width :128

Sphere evaluation symbols cup: None

SD Min Errors: 100

Hardware: CPU/GPU

4.1. Convergence Analysis

This section analyzes the convergence behavior of the DetNet and OAMP-NET networks during training, and the validation and training losses are monitored to evaluate the learning stability and the possibility of over fitting.

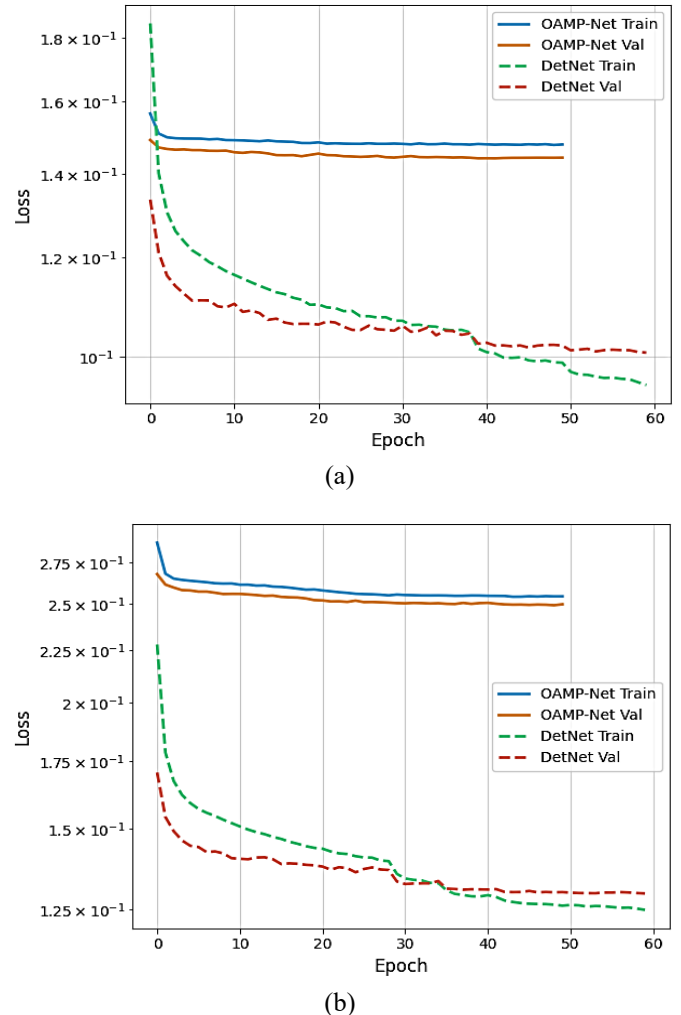
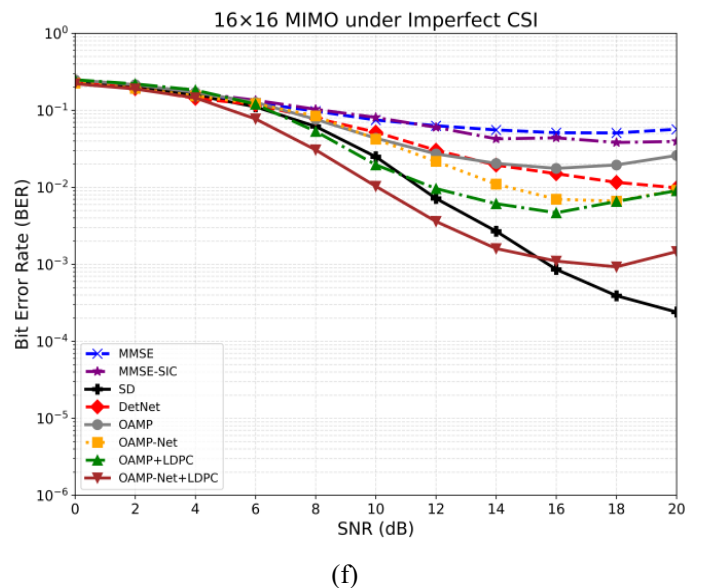
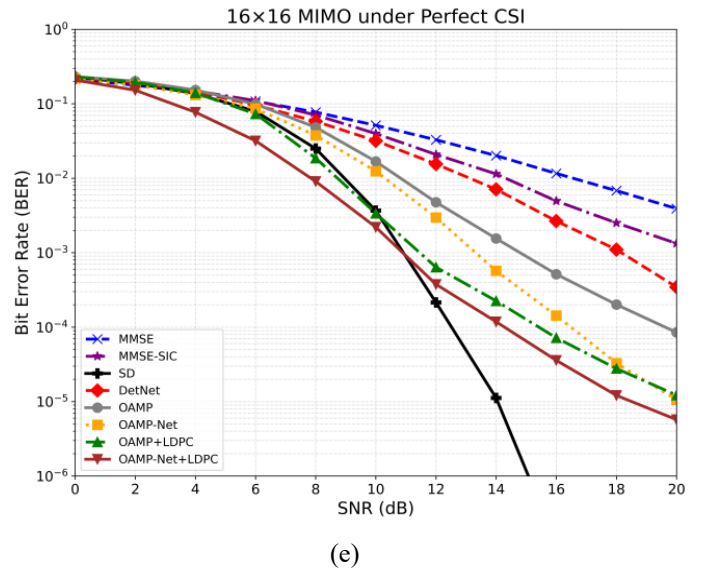
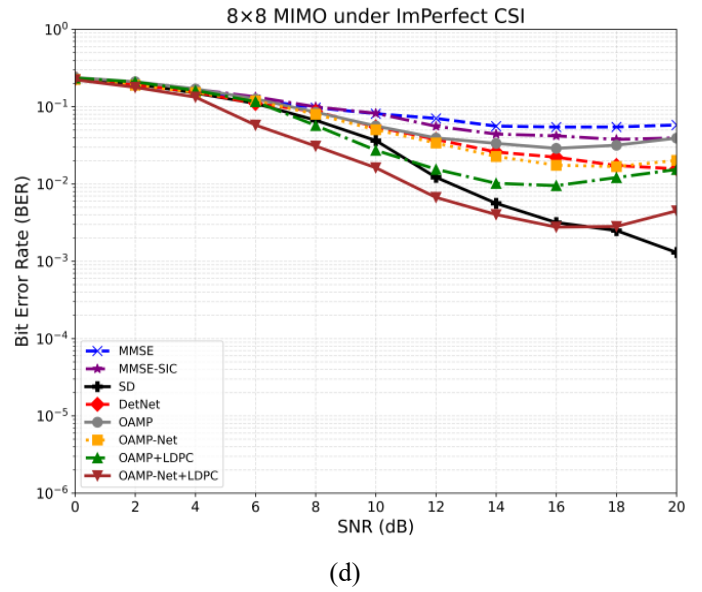
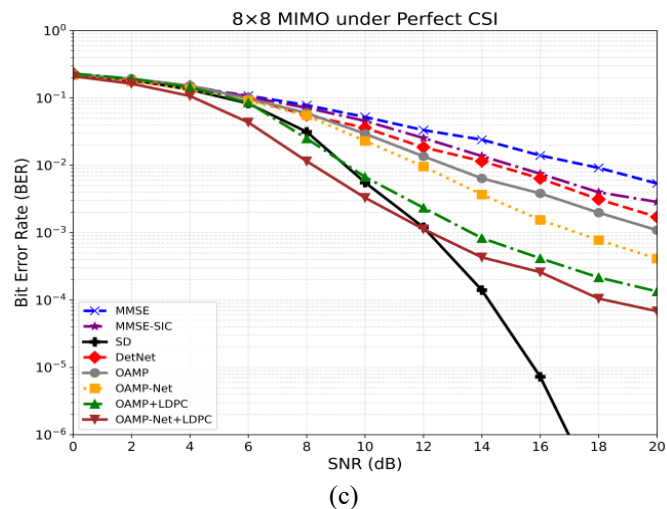
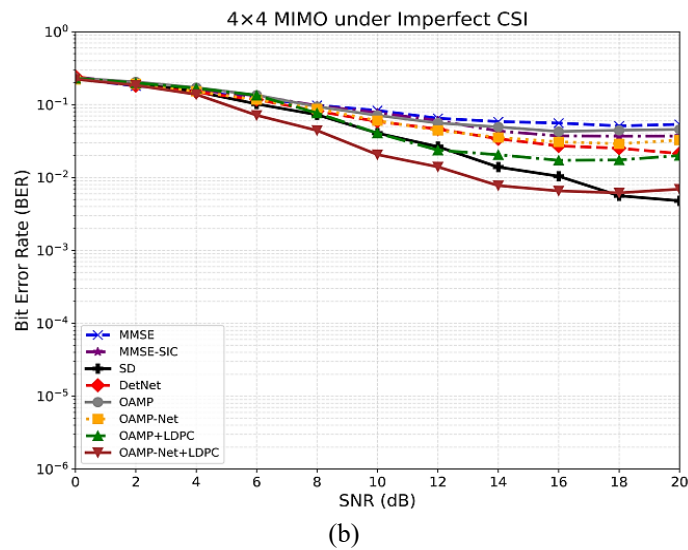
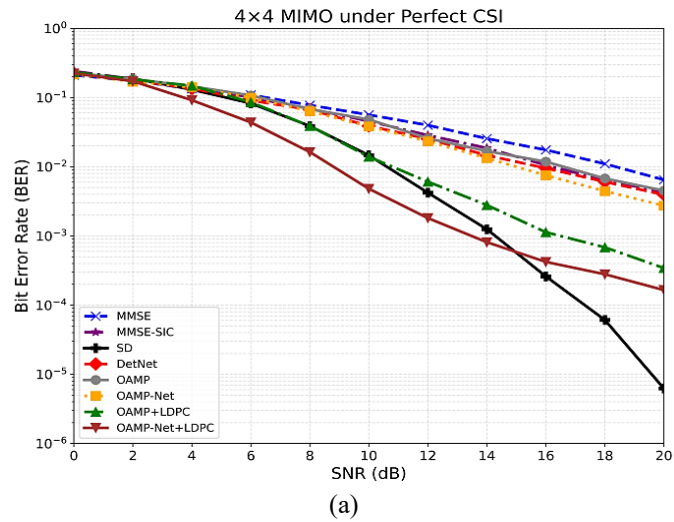


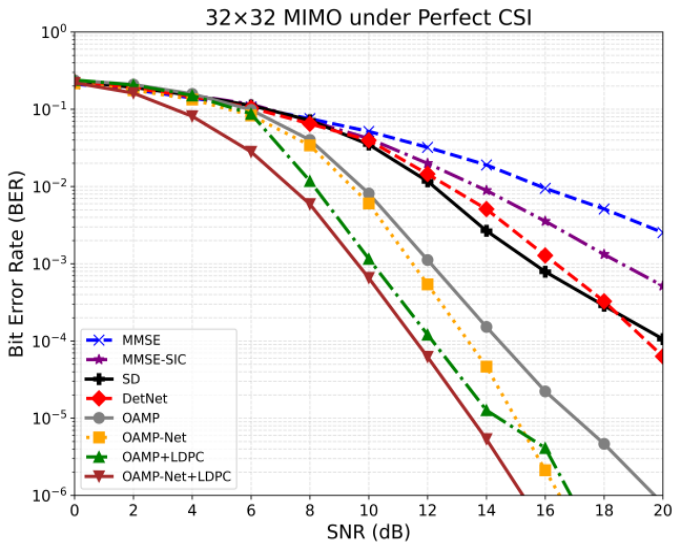
Figure 3. Convergence behavior of OAMP-Net and DetNet under (a) perfect CSI and (b) Imperfect CSI

The convergence analysis is displayed for the 8×8 MIMO configuration as a representative scenario due to its balanced detection performance and computational complexity. Figure 3 displays the convergence behavior of the DetNet and OAMP-NET networks under perfect and imperfect CSI conditions. In both cases, the training and validation losses decrease progressively with the epochs, indicating stable learning and efficient improvement without significant over fitting, as evidenced by the small difference between the training and validation curves. Under perfect CSI, both models converge to lower loss values, which reflects more accurate channel knowledge and improved learning efficiency. In contrast, imperfect CSI introduces channel estimation errors, resulting in higher final loss values and slower convergence. However, despite this degradation, the OAMP-NET and DetNet networks maintain stable convergence trends, which indicates their robustness against CSI uncertainty.

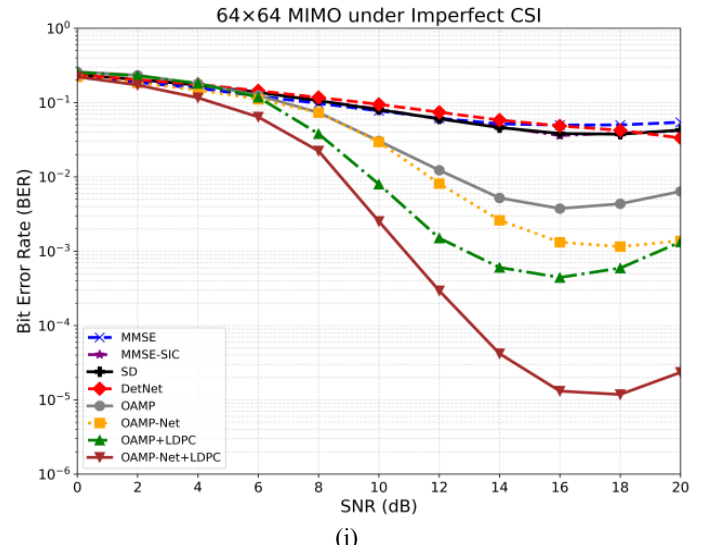
4.2. BER Performance Analysis under Perfect and Imperfect CSI

This section presents the BER analysis of the proposed system compared to other detectors under perfect and imperfect CSI conditions across different MIMO configurations.



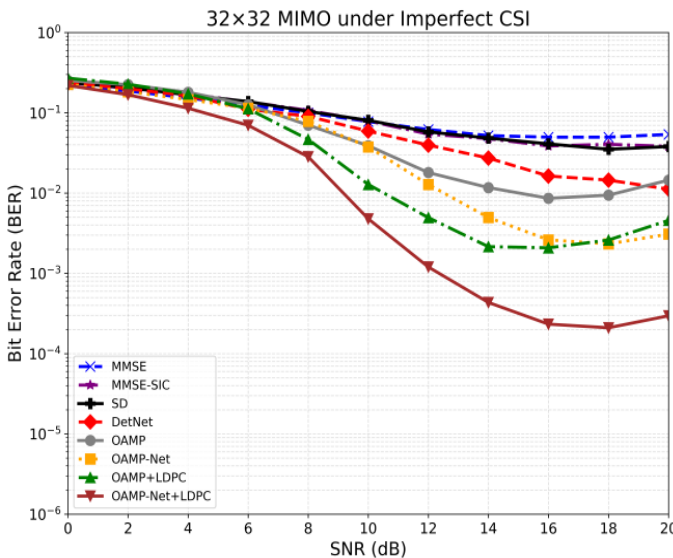


(g)

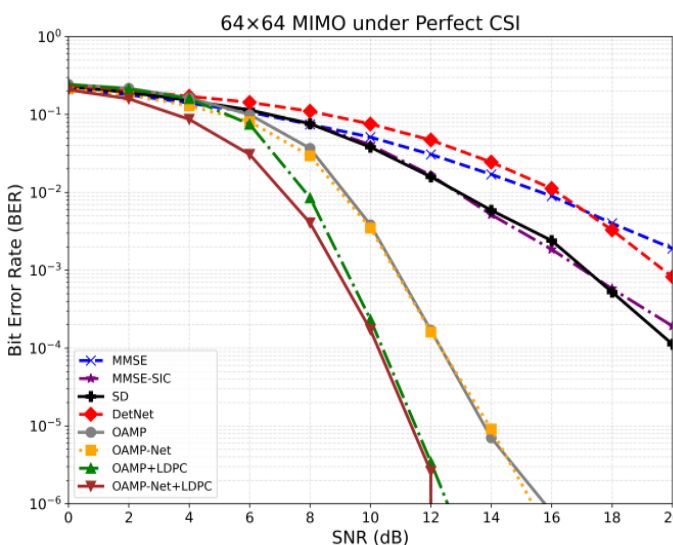


(j)

Figure 4. BER Analysis under Perfect and Imperfect CSI for Different MIMO Configurations



(h)



(i)

Figure 4 shows the BER performance of the studied detectors under perfect and imperfect CSI for different MIMO configurations ranging from 4×4 to 64×64 . In general, all detectors achieve improved BER performance as the SNR increases. However, the performance under imperfect CSI is consistently lower due to channel estimation errors which introduce residual interference and lead to noticeable error floors, especially at high SNR values, while the conventional detectors such as MMSE and MMSE - SIC is highly sensitive to imperfections channel state information. MMSE - SIC suffers from error propagation during successive interference cancellation. DetNet also suffers from performance degradation with low channel estimation accuracy. sphere decoding achieves near-optimal performance under perfect CSI, but its BER performance deteriorates under imperfect CSI this is because the channel estimation errors of the search metric, which makes the detection process more difficult. With increasing antenna dimensions Its practical performance deteriorates because the search tree grows exponentially with the number of transmitting antennas, resulting in a much larger search space and a higher computational burden, which makes its practical implementation increasingly difficult in large-scale MIMO systems and leading to performance degradation under realistic computational constraints. In contrast, OAMP-NET shows improved robustness by exploiting trainable parameters that adapt the iterative detection process to channel uncertainties. Furthermore, the incorporation of LDPC encoding significantly improves error correction capability, enabling OAMP-NET+LDPC to achieve the lowest BER among learning-based methods in all the systems studied. As the MIMO size increases from 4×4 to 64×64 , the BER performance improves due to increased spatial diversity and channel hardening effect, which enhances signal spear ability and detection reliability. These gains are particularly evident for OAMP-NET and OAMP-NET +LDPC, which can exploit additional spatial information more efficiently than conventional detectors. However, the impact of imperfect CSI more pronounced in large-scale MIMO systems because

channel estimation becomes more challenging and the accumulation of estimation errors that affect a greater number of spatial streams. Therefore, the performance gap between learning-based methods and conventional detectors widens with increasing antenna dimensions while under imperfect CSI the BER exhibits an error floor at high SNR values because channel estimation errors become the main source of performance degradation after the noise effect is significantly reduced. As a result, any additional increase in the SNR achieves only a limited improvement in performance. In the 64 x 64 MIMO system the OAMP NET+LDPC maintains excellent performance under both CSI conditions, demonstrating strong scalability and superior robustness, while conventional detectors suffer from increased sensitivity to interference and low detection accuracy. These results confirm that the combination of model-driven deep learning and channel coding provides a scalable and reliable detection framework for practical massive MIMO systems operating under realistic CSI conditions.

4.3. Statistical Validation of BER Results

To evaluate the reliability of the reported BER results, statistical validation was performed using 95% confidence intervals. Across different MIMO configurations *Table 1* shows the statistical verification of BER.

Table 1. BER Statistical Validation

Parameter	Implementation in This Study	Purpose
BER Evaluation	BER calculated using Monte Carlo simulations	Performance assessment
Confidence Interval	95% confidence interval (CI) estimated for BER values	Evaluate detection accuracy and result reliability
Statistical Reliability	Adaptive stopping criterion based on error count	Improve statistical significance
Sample Size	Variable transmitted bits according to SNR level	Reduce BER estimation variance
BER Threshold	BER reduction analyzed	Evaluate detector

Table 3. Scalability analysis under Perfect and Imperfect CSI (BER*10⁻³)

Detection Ant. Configuration		MMSE	MMSE-SIC	SD	DetNet	OAMP	OAMP-Net	OAMP+LDPC	OAMP-Net+LDPC
4 x 4	Perfect	6.47	4.27	0.00625	3.94	4.50	2.73	0.343	0.165
	Imperfect	53.6	37.0	4.79	21.3	45.7	32.6	20.0	6.92
8 x 8	Perfect	5.38	2.86	0	1.71	1.09	0.412	0.134	0.0682
	Imperfect	57.9	39.5	1.30	15.7	39.2	20.2	15.4	4.49
16x16	Perfect	3.91	1.33	0	0.345	0.0849	0.0106	0.0122	0.00572
	Imperfect	56.7	39.4	0.240	9.85	25.9	9.17	9.04	1.46
32 x 32	Perfect	2.53	0.516	0.106	0.0631	0.000781	0	0	0
	Imperfect	53.8	38.2	38.0	11.2	14.5	3.08	4.57	0.296
64 x 64	Perfect	1.90	0.192	0.112	0.819	0	0	0	0
	Imperfect	54.3	41.6	42.6	33.4	6.37	1.38	1.33	0.0234

Observation	across high-SNR regions	robustness
Validation Scope	Applied to all antenna sizes and CSI conditions	Fair comparison across scenarios

4.4. Complexity Analysis

Table 2 shows the complexity analysis for conventional and deep learning-based detection algorithms. The conventional detectors such as MMSE-SIC and MMSE exhibit polynomial complexity. SD decoding exhibits exponential complexity, making it less suitable for large-scale Massive MIMO systems. In contrast, OAMP-NET and learning based detectors provide a better trade-off between detection performance and computational scalability. Although LDPC-based schemes achieved superior BER performance, they added additional complexity to decoding due to iterative error correction, resulting greater computational burden compared to unencoded detectors.

Table 2. Computational Complexity Analysis

Detectors	Computational Complexity
MMSE	$O(N_{rx}^3 + N_{rx}^2 N_{tx})$
MMSE-SIC	$O(N_{tx} N_{rx}^3)$
Sphere decoding SD	Exponential / $O(D K A)$
DetNet	$O(L(H_d^2 + H_d N_{tx}))$
OAMP	$O(T(N_{rx}^3 + N_{rx}^2 N_{tx}))$
OAMP-Net	$O(T(N_{rx}^3 + N_{rx}^2 N_{tx}))$
OAMP + LDPC	$O(T(N_{rx}^3 + I LDPC E))$
OAMP-Net + LDPC	$O(T(N_{rx}^3 + I LDPC E))$

4.5. Scalability Analysis

This section evaluates the scalability of the detectors by increasing the dimensions of the MIMO system. The analysis focuses on the stability of the (BER) with increasing antenna size, demonstrating the capability of each detector to maintain performance in large-scale MIMO systems. *Table 3* display BER values at SNR = 20dB or all detection algorithms to evaluate the scalability across different antenna configurations and under different channel conditions.

The Scalability analysis shows that increasing the antenna size from 4×4 to 64×64 does not negatively affect the performance of advanced detectors such as OAMP-NET and LDPC-based systems, which maintain very low BER values under perfect and imperfect CSI conditions. This indicates strong scalability and robustness in massive MIMO environments. In contrast, conventional detectors, especially MMSE-SIC and MMSE, show a gradual degradation in performance, while both SD and DetNet significantly deteriorates when using larger antennas due to increased computational complexity and channel estimation error sensitivity. The proposed OAMP-NET+LDPC approach shows the best scalability among all evaluated detectors.

4.6. Generalization Analysis

This section presents an evaluation of the generalization capability of the OAMP-NET detector under both perfect and imperfect channel CSI conditions in *figure 5* and *figure 6* respectively. The analysis investigates the robustness of the trained model when tested on correlated channel environments and unseen SNR values that were not included during training.

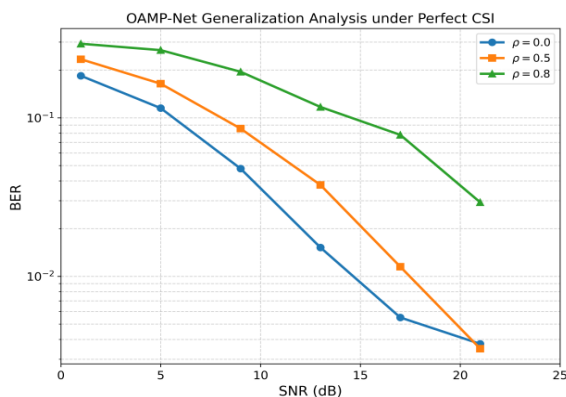


Figure 5. OAMP-NET Generalization Analysis under Perfect CSI

Figure 5 shows that the OAMP-NET is able to successfully generalize to unseen SNR values while maintaining stable detection performance. As the SNR increases, the BER decreases significantly in all channel conditions, which confirms the robustness of the trained model. In addition, the results indicate that channel correlation negatively affects in the system performance, as the lowest values of BER are achieved in the case of the uncorrelated channel, $\rho = 0$, while higher correlation levels, $\rho = 0.5$, $\rho = 0.8$, lead to Noticeable deterioration in BER due to the reduction in spatial diversity and increased difficulty in separating signals. Overall, the OAMP-NET maintains reliable performance across different channel correlation scenarios, demonstrating good generalization ability.

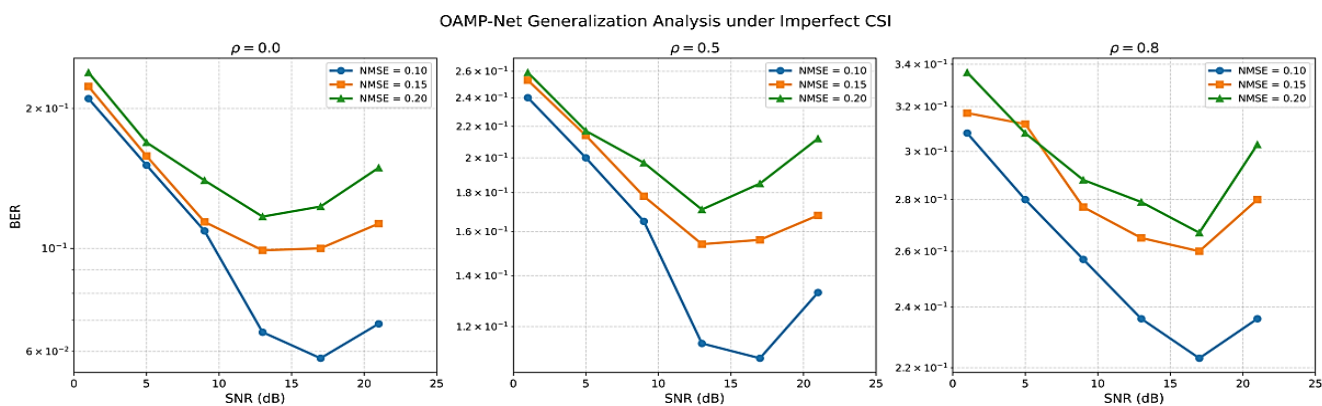


Figure 6. OAMP-NET Generalization Analysis under Imperfect CSI

While *figure 6* shows that the OAMP-NET detector maintains stable detection capability under unseen SNR conditions and different channel environments. However, the BER performance deteriorates with increasing channel estimation error (Normalized Mean Square Error NMSE) and the channel correlation coefficient ρ for low correlation channels ($\rho=0$) the detector still achieves acceptable BER performance, especially at medium and high SNR values. In contrast, channels with high correlation ($\rho=0.5$, $\rho = 0.8$) lead to a significant deterioration in detection accuracy due to the loss of spatial diversity and increased interference among antennas in addition, increasing the CSI error NMSE from 0.10 to 0.20 leads to a significant increase in the BER across all SNR ranges, which indicates that the quality of the channel estimation significantly affects the robustness of the OAMP NET, but despite this degradation the detector maintains a stable performance trend, which confirms its ability to generalize under conditions of imperfect CSI.

4.7. Ablation study

This section presents an analytical study under perfect and imperfect CSI conditions. The objective of this analysis is to evaluate the effect of the unfolded network depth on the detection performance, model complexity, and training behavior. Different numbers of unfolded layers were examined to analyze the trade-off between improving the BER and computational complexity.

Table 4. Ablation study under Perfect CSI

Number of Unfolded Layers	Trainable Parameters	BER at 12dB	Validation Loss
5	10	2.29×10^{-2}	1.867×10^{-1}
10	20	2.16×10^{-2}	1.841×10^{-1}
15	30	2.19×10^{-2}	1.867×10^{-1}
20	40	2.29×10^{-2}	1.796×10^{-1}

The ablation results in *table 4* show that increasing the number of layers of the unfolded OAMP-NET network improves the leaning capability of the networks. The 10-layer configuration achieved the best BER performance at 12 dB, while the deeper models reduced the validation loss slightly, but did not significantly improve the BER. This indicates that a moderate network depth provides a good trade-off between detection accuracy and computational complexity.

Table 5. Ablation Study under Imperfect CSI

Layers	Trainable Parameters	BER at 12 dB	Validation Loss
5	10	4.71×10^{-2}	2.996×10^{-1}
10	20	4.79×10^{-2}	3.042×10^{-1}
15	30	5.03×10^{-2}	3.051×10^{-1}
20	40	4.41×10^{-2}	2.991×10^{-1}

The ablation results under imperfect CSI (NMSE = 0.05) in *table 5*. show that increasing the number of layers of the unfolded OAMP NET network slightly improves the robustness of detection against channel estimation errors, as the 20-layer model achieved the best performance in terms of BER and verification loss, which indicates that increasing the convolution depth reduces the uncertainty in CSI better. However, the performance differences between the configurations remain relatively small compared to the increase in model complexity.

Despite the promising BER performance achieved by the proposed OAMP-NET+LDPC model there are still several practical challenges, as the computational complexity and implementation time increase significantly when expanding the system to include larger MIMO configurations with higher antenna dimensions. In addition, the training process requires large computational resources and longer convergence time. Therefore, further improvement is still needed to enhance scalability and reduce the implementation cost in large-scale massive MIMO systems.

5. CONCLUSION

We have developed a Massive MIMO system that integrates the LDPC code with a detector based on a model-driven deep learning network, where the power of the deep learning used, represented by the OAMP-NET detection algorithm, has been exploited, which is characterized by ease and speed of training due to the small number of learnable parameters, which leads to improving the LLRS values entering the LDPC decoder and thus improving the performance of the decoding process, as the results present the strength of the proposed system in reducing the BER rate under both perfect and imperfect CSI and the results show that the scalability of the proposed system across different number of antenna configurations. The main strengths of the proposed method lie in the low number of trainable parameters, 20 parameters for 10 layers, which is much less than fully data-driven neural detectors that usually require thousands to millions of parameters. The computational complexity remains on the same order as conventional OAMP, making this method suitable for large-scale MIMO systems.

Author contributions: Saja Abdul Karim proposed and supervised the problem statement, the work on the concept and work funding. Marwa Al-Sultani developed the methodology also verified and performed the analytical methods.

Conflicts of interest: There are no competing interests to declare.

REFERENCES

- [1] M. Al-Sultani, W. Q. Mohamed, and M. Huiyi, "Study on various antenna configurations," in 2018 2nd International Symposium on Multidisciplinary Studies and Innovative Technologies (ISMSIT), 2018, pp. 1-5.
- [2] M. Al-Sultani, H. R. Hatem, and W. Q. Mohamed, "Performance enhancement of audio transmission based on LMMSE method," Indonesian Journal of Electrical Engineering and Computer Science, vol. 21, pp. 903-910, 2021.
- [3] H. R. HATEM, A. M. AHMED, and M. AL-SULTANI, "IMPROVING RELIABILITY, CAPACITY, AND SECURITY OF AUDIO TRANSMISSION BASED ON MULTIPLE ANTENNAS USING MGSTC TECHNOLOGIES," Journal of Engineering Science and Technology, vol. 17, pp. 1247-1264, 2022.
- [4] M. A. Albreem, K. A. Alnajjar, and A. J. Almasadeh, "Massive mimo detectors based on deep learning, stair matrix, and approximate matrix inversion methods," IEEE Access, vol. 11, pp. 100268-100283, 2023.
- [5] G. Omondi and T. O. Olwal, "A DNN-Based MIMO Signal Detector Using Transformer Architecture for Next-Generation Wireless Networks*," Journal of Information and Intelligence, 2025.
- [6] A. Kumar, N. Gaur, and A. Nanthaamornphong, "Signal detection of massive MIMO systems using LSTM-based signal detectors for beyond 5G radio," Alexandria Engineering Journal, vol. 127, pp. 760-770, 2025.
- [7] H. He, C.-K. Wen, S. Jin, and G. Y. Li, "Model-driven deep learning for MIMO detection," IEEE Transactions on Signal Processing, vol. 68, pp. 1702-1715, 2020.
- [8] H. He, C.-K. Wen, S. Jin, and G. Y. Li, "A model-driven deep learning network for MIMO detection," in 2018 IEEE Global Conference on Signal and Information Processing (GlobalSIP), 2018, pp. 584-588.

- [9] W. Q. Mohamed, M. Al-Sultani, and H. R. Hatem, "New 2-D interleaving grouping LBC applied on image transmission," *International Journal of Electrical and Computer Engineering (IJECE)*, vol. 11, pp. 4241-4249, 2021.
- [10] W. Ullah, F. Yang, and D. N. K. Jayakody, "OTFS modulated massive MIMO with 5G NR LDPC coding: Trends, challenges and future directions," *Computer Networks*, vol. 254, p. 110751, 2024.
- [11] M. Marques da Silva, R. Dinis, and G. Martins, "On the performance of LDPC-coded massive MIMO schemes with power-ordered NOMA techniques," *Applied Sciences*, vol. 11, p. 8684, 2021.
- [12] H. J. Park and J. W. Lee, "Design of LDPC coded multi-user massive MIMO systems with MMSE-based iterative joint detection and decoding," *IEEE Access*, vol. 11, pp. 125492-125510, 2023.
- [13] M. M. Islam, M. A. Islam, and M. F. Ahmed, "A DNN-based 5G MIMO system adopting a mix of tactics," *Discover Electronics*, vol. 2, p. 15, 2025.
- [14] M. Sy, "Demystifying 5G Polar and LDPC Codes: A Comprehensive Review and Foundations," *arXiv preprint arXiv:2502.11053*, 2025.



© 2026 by Saja Abdul Karim Anwar, and Marwa Al-Sultani. Submitted for possible open access publication under the terms and conditions of the Creative Commons Attribution (CC BY) license (<http://creativecommons.org/licenses/by/4.0/>).